

Are your MRI contrast agents cost-effective?

Learn more about generic Gadolinium-Based Contrast Agents.



FRESENIUS  
KABI

caring for life

**AJNR**

**Clinical Correlates of White Matter Blood Flow Perfusion Changes in Sturge-Weber Syndrome: A Dynamic MR Perfusion-Weighted Imaging Study**

Y. Miao, C. Juhász, J. Wu, B. Tarabishy, Z. Lang, M.E. Behen, Z. Kou, Y. Ye, H.T. Chugani and J. Hu

This information is current as of April 17, 2024.

*AJNR Am J Neuroradiol* published online 30 June 2011  
<http://www.ajnr.org/content/early/2011/06/30/ajnr.A2540>

ORIGINAL  
RESEARCH

Y. Miao  
C. Juhász  
J. Wu  
B. Tarabishy  
Z. Lang  
M.E. Behen  
Z. Kou  
Y. Ye  
H.T. Chugani  
J. Hu



# Clinical Correlates of White Matter Blood Flow Perfusion Changes in Sturge-Weber Syndrome: A Dynamic MR Perfusion-Weighted Imaging Study

**BACKGROUND AND PURPOSE:** Low brain tissue perfusion due to abnormal venous drainage is thought to be a central mechanism of brain damage in SWS. Here, HR-PWI was used to quantify WM perfusion abnormalities and to correlate these with brain atrophy and clinical variables.

**MATERIALS AND METHODS:** Fourteen children (age range, 0.8–10.0 years) with unilateral SWS underwent MR imaging examinations, including HR-PWI. rCBV, rCBF, and MTT in the affected WM and in contralateral homotopic WM were measured. AI for each perfusion parameter was correlated with age, brain atrophy, and motor and seizure variables as well as IQ.

**RESULTS:** Increased perfusion was seen in the affected hemisphere in 5 children and decreased perfusion in 9 children. Brain atrophy was more severe in the low-perfusion group ( $P = .01$ ) and was related to both CBF-AI and CBV-AI ( $r = -0.69$ ,  $P = .007$ ;  $r = -0.64$ ,  $P = .014$ , respectively). Older children had lower CBV values on the affected side ( $r = -0.62$ ,  $P = .02$ ). Longer duration of epilepsy was related to lower CBF (more negative CBF-AI,  $r = -0.58$ ,  $P = .03$ ) and low CBV ( $r = -0.55$ ,  $P = .04$ ) on the affected side. Lower perfusion was associated with more frequent seizures (rCBF-AI:  $r = -0.56$ ,  $P = .04$ ; rCBV-AI:  $r = -0.63$ ,  $P = .02$ ).

**CONCLUSIONS:** Increased perfusion in the affected cerebral WM may indicate an early stage of SWS without severe brain atrophy. Decreased perfusion is associated with frequent seizures, long duration of epilepsy, and brain atrophy.

**ABBREVIATIONS:** AI = asymmetry index; AI<sub>c</sub> = calculated asymmetry index; AI<sub>s</sub> = hemispheric perfusion parameter; A<sub>mr</sub> = age at MR examination; A<sub>sz</sub> = age at first seizure; BA = brain atrophy; CBF = cerebral blood flow; CBV = cerebral blood volume; Cont = contralateral (to angioma); HR-PWI = high-resolution perfusion-weighted imaging; Ipsi = ipsilateral; IQ = intelligence quotient; MTT = mean transit time; PET = positron-emission tomography; PHT = phenytoin; PWI = perfusion-weighted imaging; rCBF = relative cerebral blood flow; rCBV = relative cerebral blood volume; rHP = relative high perfusion; rLP = relative low perfusion; rMTT = relative mean transit time; ROI = region of interest; SPECT = single-photon emission CT; SPIN = Signal intensity Process in Neuroimaging; SWS = Sturge-Weber syndrome; T1WI = T1-weighted imaging; T2WI = T2-weighted imaging; WM = white matter

As a sporadic neurocutaneous disorder, SWS is classically characterized by a facial port-wine stain in the trigeminal nerve distribution, a leptomeningeal angioma, and ocular abnormalities.<sup>1</sup> Progressive neurologic symptoms, including seizures, visual field defects, and hemiparesis, are often present in children with SWS and are probably the result of hypoxia-induced cortical injury.<sup>2</sup> In contrast to the prominent pathologic abnormalities in the cortex, including astrogliosis, atrophy, and perivascular calcifications, the WM shows relatively

less structural abnormality on conventional MR imaging. Nevertheless, recent MR studies have recognized that structural changes in WM may play a major role in the clinical manifestations of SWS, such as cognitive impairment.<sup>3-6</sup>

Abnormal cortical drainage and venous stasis result from an anomalous venous plexus over the cerebral surface in patients with SWS, leading to impaired cortical perfusion and ischemia, further aggravated by repetitive and progressively worsening seizures.<sup>2</sup> Nevertheless, it is unclear whether abnormal blood perfusion in the affected WM directly contributes to the clinical features of SWS. Previous functional neuroimaging, such as PET and SPECT studies have found that blood flow deficit in the affected cortical regions was common in SWS, probably contributing to neurologic impairment.<sup>7-9</sup> Recent dynamic contrast-enhanced MR PWI studies also have shown similar results.<sup>10-12</sup> In addition, a few patients have been reported to show increased blood flow in the affected cortex as detected by PWI or SPECT. Those patients typically had recent seizure onset.<sup>7,13</sup> However, little research has focused on the hemodynamics in WM and its relation to the clinical features of SWS. Here, we combined PWI and conventional MR imaging to quantify WM perfusion in a prospectively recruited group of children with unilateral SWS. Fur-

Received October 14, 2010; accepted after revision November 21.

From the Department of Radiology (Y.M., J.W., Z.L.), First Affiliated Hospital, Dalian Medical University, Dalian, Liaoning, China; Departments of Pediatrics and Neurology (C.J., M.E.B., H.T.C.), Translational Imaging Center, Children's Hospital of Michigan, Wayne State University, Detroit, Michigan; and Department of Radiology (Y.M., B.T., Z.K., Y.Y., J.H.), Wayne State University, Detroit, Michigan.

This work was supported by the National Institutes of Health (grant NS041922; principle investigator: C.J.) and Excellent Talents Plan of Liaoning Institution of Higher Education in China (grant 2009R16; principle investigator: J.W.).

Please address correspondence to Jiani Hu, MD, Department of Radiology, Wayne State University, 3990 John R Rd, Detroit, MI 48202; e-mail: jhu@med.wayne.edu



Indicates open access to non-subscribers at [www.ajnr.org](http://www.ajnr.org)



Indicates an article with supplemental on-line tables.

DOI 10.3174/ajnr.A2540

thermore, we paid particularly close attention to the correlation between perfusion parameters in WM and some putative impacting factors, including age, brain atrophy, and seizure variables, as well as the potential relation between WM perfusion status and motor as well as cognitive functions.

## Materials and Methods

### Subjects

In this study, data of 14 children (8 girls and 6 boys; age range, 0.8–10.0 years; median age, 4.0 years) with unilateral SWS were analyzed, selected from 45 children recruited prospectively for a clinical and neuroimaging study of children with SWS between 2003 and 2010. The present study was based on the following inclusion criteria<sup>5</sup>: 1) diagnosis of SWS with unilateral brain involvement based on clinical and imaging features (conventional MR imaging as well as fluorodeoxyglucose PET, performed within 24 hours of the MR imaging studies) and 2) the availability of good quality PWI images. Patients were excluded if they had bilateral brain involvement, because an unaffected hemisphere must be present to make a meaningful comparison between sides on PWI. Of the 14 children, 13 had a history of seizures, and 7 suffered from hemiparesis of varying degrees and extent. Online Table 1 shows the clinical data, including  $A_{mr}$ ,  $A_{sz}$ , average seizure frequency, duration of epilepsy, and full scale IQ score.

In addition, 10 healthy adults (5 men and 5 women; age range, 22–47 years; median age, 34 years) were recruited as controls to establish normal perfusion parameter asymmetries between hemispheres. Exclusion criteria for this group included a history of a neurologic or psychiatric condition, head trauma with loss of consciousness for >5 minutes, a habit of drug or alcohol abuse, brain surgery, as well as focal hyperintensity in the brain on T2-weighted images. The study was approved by the Wayne State University Human Investigation Committee, and informed consent of the parent or legal guardian was obtained.

### MR Imaging Protocol

All children with SWS underwent an MR imaging examination by using a Sonata 1.5T MR scanner (Siemens, Erlangen, Germany) with a standard head coil. Patients <7 years of age were sedated with pentobarbital (3 mg/kg) followed by fentanyl (1  $\mu$ g/kg). The MR imaging protocol included an axial 3D gradient-echo T1-weighted acquisition (TR, 20 ms; TE, 5.6 ms; flip angle, 25°; and voxel size, 1.0  $\times$  0.5  $\times$  2.0 cm<sup>3</sup>), an axial T2-weighted turbo spin-echo acquisition (TR, 5020 ms; TE, 106 ms; voxel size, 1.0  $\times$  1.0  $\times$  6.0 cm<sup>3</sup>), susceptibility-weighted imaging, followed by dynamic contrast-enhanced HR-PWI and a postgadolinium T1-weighted acquisition (by using the same imaging parameters as the first T1-weighted acquisition) in all patients. The HR-PWI data were obtained by using a 2D gradient-echo echo-planar sequence with TR, 2200 ms; TE, 98 ms; flip angle, 60°; and section thickness, 4 mm. The FOV was 256  $\times$  256 mm and the matrix was 512  $\times$  512. The scan was run 50 times. The contrast agent gadolinium-DTPA (Magnevist; Berlex, Wayne, New Jersey) was bolus injected via a peripheral vein on one of the hands by a power injector (Spectris MR injection system; Medrad, Warrendale, Pennsylvania) with a dose of 0.1 mmol/kg body weight at a rate of 2 mL/s. On PWI, a smaller voxel size of 0.5  $\times$  0.5  $\times$  4.0 mm<sup>3</sup>, compared with those published previously,<sup>10–12</sup> was obtained to improve the ability of detecting subtle structures in cerebral parenchyma; therefore, the PWI method used here is termed HR. The 10 control subjects also underwent HR-PWI with the same protocol.

### MR Data Processing

**BA Estimation.** All acquired datasets were transferred to a PC workstation for postprocessing by using SPIN software developed in-house.<sup>14,15</sup> The affected hemisphere was defined according to characteristic findings including leptomeningeal angioma and/or transmedullary veins as well as enlarged venous plexus on the contrast enhanced T1WI. T2WI was used to measure the degree of BA because of its superior image contrast. Two neuroradiologists manually traced the areas of the affected hemisphere on T2WI in all selected sections (but a minimum of 3 consecutive sections) with vascular involvement as evidenced by contrast-enhanced T1WI. All sections showing involvement with abnormal vessels on contrast-enhanced T1WI were regarded as regions to be measured.

A hemispheric ROI was drawn along the surface of cortex and midline structures. The ROI included all cortex, WM, and ventricle in a hemisphere in a section. In the same way, contralateral hemispheric areas also were manually delineated in all affected sections. Moreover, the ipsilateral (affected) and contralateral hemispheric volumes were respectively obtained by calculating the sum of all affected sections. BA-AIs were calculated by formula 1<sup>16</sup>:

$$1) \text{ BA-AI} = \frac{(\text{ipsilateral volume} - \text{contralateral volume})}{([\text{ipsilateral volume} + \text{contralateral volume}]/2)}.$$

**PWI Analysis.** A series of perfusion parameter maps were post-processed from MR perfusion raw data based on tracer kinetic methods,<sup>17</sup> including rCBV, rCBF, and MTT, in SPIN software. Among these indices, rCBF values more directly and specifically reflect the blood flow status in the brain tissue. As a result, the rCBF map was chosen for comparing the cerebral perfusion between the 2 (affected versus unaffected) hemispheres. rCBF, rCBV, and rMTT values in the affected WM, defined by the presence of abnormally enhancing vessels and/or leptomeningeal venous angiomatosis, and contralateral homotopic WM were manually measured by 2 neuroradiologists. Three ROIs, 20–40 voxels, were placed on every section in the affected and contralateral WM. On the CBF map, vessels and cortex are colored red and green, respectively, and WM is colored blue, allowing for accurate placement of ROIs over WM, while avoiding inclusion of vessels, cortex, and ventricle (Fig 1). Perfusion parameters were measured in all affected regions based on abnormal features on contrast-enhanced T1WI, including leptomeningeal angioma and/or dilated transmedullary veins, the very same features used to define involvement when calculating brain atrophy ratios as described above. The final values quoted were the mean of the measurements in all affected sections, yielding hemispheric perfusion parameter  $AI_s$ , calculated based on formula 2.

$$2) \text{ CBF-}AI_s = (\text{CBFI} - \text{CBFC})/((\text{CBFI} + \text{CBFC})/2),$$

$$\text{CBV-}AI_s = (\text{CBVI} - \text{CBVC})/((\text{CBVI} + \text{CBVC})/2),$$

$$\text{MTT-}AI_s = (\text{MTTI} - \text{MTTC})/((\text{MTTI} + \text{MTTC})/2).$$

CBF- $AI_s$ , CBV- $AI_s$ , and MTT- $AI_s$  are the asymmetry indices of CBF, CBV, and MTT in SWS patients; CBFI, CBVI, and MTTI indicate the CBF, CBV, and MTT values in WM ipsilateral to the angioma; and CBFC, CBVC, and MTTC are the perfusion values in the contralateral hemisphere, measured in homotopic regions.

Among the control group, the same 3 perfusion parameters also were measured in bilateral frontal, parietal, temporal, and occipital WM. The ROIs were placed in deep frontal WM, posterior centrum

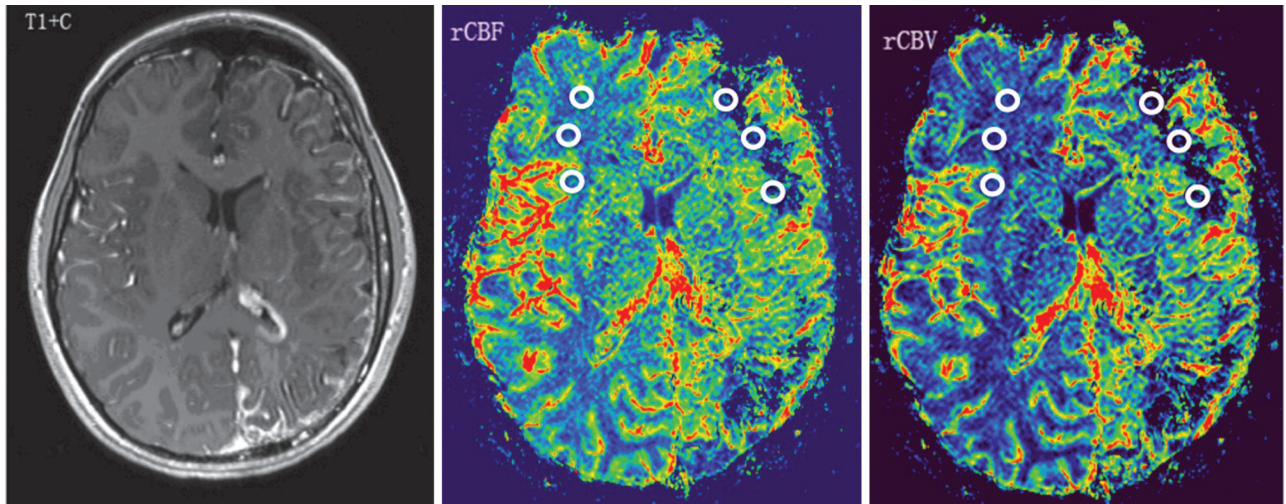


**Fig 1.** A 10-year-old girl with developmental delay (IQ = 55) and monthly seizures (patient 3 in On-line Tables 1 and 2). Contrast-enhanced T1WI (T1+C) shows left hemisphere volume loss and characteristic leptomeningeal enhancement in the same region, as well as a prominent left choroid plexus. PWI demonstrates decreased rCBF and rCBV ( $CBF-AI_s = -0.67$ ,  $CBV-AI_s = -0.52$ ) in the left frontal and occipital WM regions, underlying the leptomeningeal angiomas. Regions of interest placed on the affected left frontal WM and contralateral homotopic region are demonstrated.

semiovale, optic radiations, and WM adjacent to temporal horn of the lateral ventricle. ROIs were 20–40 voxels. Measurements were made section by section by placing ROIs on WM in the areas described above. The mean and SD of perfusion asymmetry indices ( $CBF-AI_c$ ,  $CBV-AI_c$  and  $MTT-AI_c$ ) were calculated, thus creating a reference to determine the perfusion contrast between hemispheres in SWS cases, according to formula 3:

$$3) \quad CBF-AI_c = (CBFR - CBFL) / ((CBFR + CBFL) / 2),$$

$$CBV-AI_c = (CBVR - CBVL) / ((CBVR + CBVL) / 2),$$

$$MTT-AI_c = (MTTR - MTTL) / ((MTTR + MTTL) / 2).$$

$CBF-AI_c$ ,  $CBV-AI_c$ , and  $MTT-AI_c$  are the asymmetry indices of CBF, CBV, and MTT between hemispheres in controls; CBFR, CBVR, and MTTR indicate the CBF, CBV, and MTT values in the right WM; and CBFL, CBVL, and MTL are the perfusion values in the left hemisphere, measured in homotopic regions.

### Assessment of Cognitive Functions

All children received a comprehensive neuropsychologic assessment within 1 day of the MR imaging studies, administered by a pediatric neuropsychologist. Neuropsychological testing for global intellectual functioning (IQ) was performed in the morning, before sedation for imaging, by using previously detailed protocols in all children >18 months of age ( $n = 13$ ).<sup>3,5</sup>

### Seizure Frequency Score

Because seizure frequency could not be determined with exact accuracy, a seizure frequency score was calculated based on a scoring system proposed by Engel et al.<sup>18</sup> We have used a simplified version of this scoring system according to a 5-point scale as follows: 1,  $\leq 1$  seizure per year; 2, 2–11 seizures per year; 3, 1–3 seizure(s) per month; 4, 1–6 seizure(s) per week; and 5:  $\geq 1$  seizure(s) per day.

### Statistical Analysis

Reliability of measurements was first investigated with a desired correlation coefficient value of  $>0.90$ <sup>19</sup> by single measure intraclass correlation after the rCBF, rCBV, rMTT, and BA-AI values had been

measured twice by 2 neuroradiologists for all the subjects. Group comparisons of perfusion variables and AIs were performed by Mann-Whitney U-test by using SPSS (release 16.0; SPSS, Chicago, Illinois), due to the non-normality distribution occurring in part of the data. Relationships between these perfusion values and  $A_{mr}$ , BA-AI, seizure frequency, duration of epilepsy,  $A_{sz}$ , and IQ scores were determined by nonparametric Spearman rank correlation. All statistical analyses were performed with a 0.05 level of significance.

## Results

### Intraclass and Interclass Reliability of Hemispheric Atrophy and Perfusion Measurements

The intraclass and interclass reliability of rCBF, rCBV, and rMTT in the SWS cases and controls and BA-AI values in the SWS subjects were beyond our target value of 0.90, varying from 0.93 to 0.98 and from 0.94 to 0.97, respectively.

### Perfusion Asymmetries: High Perfusion and Low Perfusion in the Affected Hemisphere

Among the control group, the mean and SD of  $CBF-AI$ ,  $CBV-AI$ , and  $MTT-AI$  was  $0.004 \pm 0.006$ ,  $0.009 \pm 0.014$ , and  $0.008 \pm 0.008$ , respectively. A cutoff of 2 SDs above and below the mean for  $CBF-AI$  (0.008,  $-0.016$ ; ie,  $<2\%$  asymmetries in normal brain) was defined as the normal range.  $CBF-AI$  values falling outside this range for the SWS group were regarded as abnormal.

In the SWS group,  $CBF-AI_s$  varied between  $-0.82$  and  $+0.39$ , whereas  $CBV-AI_s$  varied between  $-0.67$  and  $+0.69$ . All  $CBF-AI_s$  values were considerably outside the normal range (the smallest AI was  $-0.12$ , consistent with a 12% asymmetry), and patients were divided into 2 subgroups according to their  $CBF-AI_s$  values: an rLP group (negative  $CBF-AI_s$ , indicating abnormally low perfusion on the angioma side;  $n = 9$ ; Fig 1) and an rHP group (positive  $CBF-AI_s$ , increased perfusion on the angioma side;  $n = 5$ ; Fig 2). Detailed results are listed in On-line Table 2. It should be noted that 4 of the 5 children with high perfusion had a history of seizures, but all 4



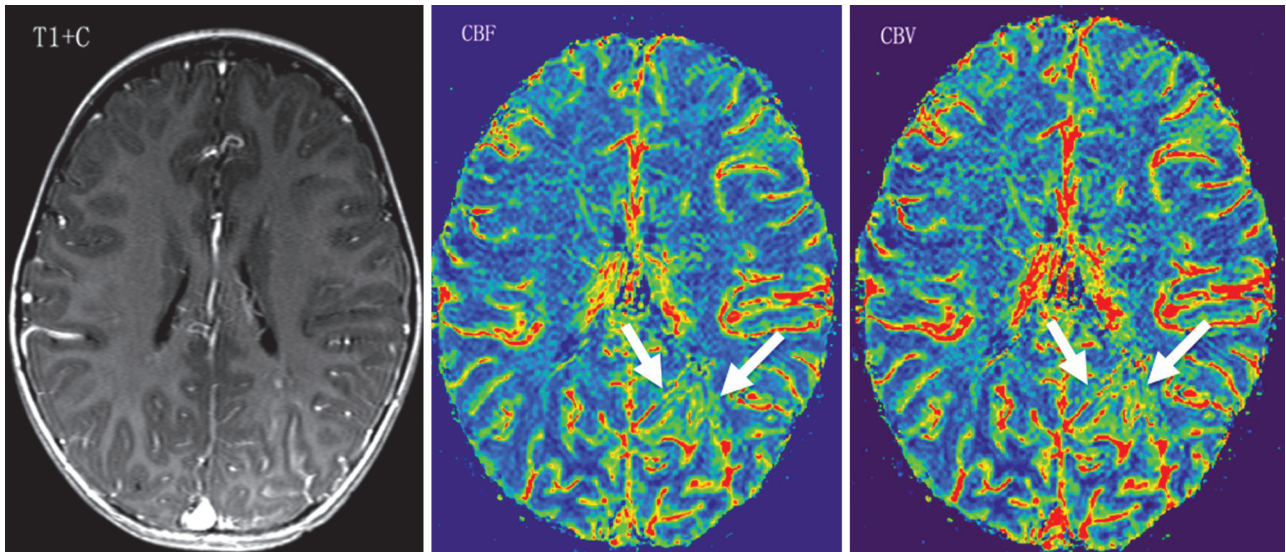


**Fig 2.** A 2-year-old girl with normal cognitive development (IQ = 105) and no seizures. Contrast-enhanced T1WI (T1+C) shows leptomeningeal enhancement in the left occipital lobe. PWI demonstrates increased WM rCBF and rCBV (CBF-AI = 0.26, CBV-AI = 0.24) in the involved region (arrows).

were free of clinical seizures for at least 4 months before the MR imaging scan.

BA-AI in the rLP group was significantly lower (mean,  $-0.15$ ; ie, an average of 15% volume decrease) than in the rHP group ( $-0.04$ ,  $P = .01$ ), indicating more severe atrophy in the affected brain regions of the rLP group on the side affected by the venous angioma. In contrast, there was no significant difference in age ( $A_{mr}$ ) or IQ between the groups, though there was a moderate trend for lower age in the rHP group, compared with the age of children in the rLP group (mean age, 3.6 versus 5.3 years;  $Z = -1.41$ ,  $P = .16$ ).

#### **Correlation between Perfusion Status and Age, Atrophy, Hemiparesis, and IQ**

A significant negative correlation was found between the age at MR imaging examination and CBV value on the affected side ( $r = -0.62$ ,  $P = .02$ ). There was a trend toward a negative correlation with CBF-AI<sub>s</sub> ( $r = -0.50$ ,  $P = .065$ ). BA-AI values also demonstrated a significant positive correlation with CBF-AI<sub>s</sub> as well as CBV-AI<sub>s</sub> ( $r = 0.69$ ,  $P = .007$ ;  $r = 0.64$ ,  $P = .014$ , respectively). Patients with hemiparesis ( $n = 7$ ) had more severe brain atrophy AIs than those with no paresis (BA-AI =  $0.17 \pm 0.10$  versus  $0.05 \pm 0.06$ , respectively); however, perfusion variables were not different between the 2 subgroups ( $P > .10$  in all comparisons). Also, there was no relation between perfusion values/asymmetries and IQ of children ( $P > .60$  in all comparisons), though all 3 patients with IQ  $<70$  ( $>2$  SD below normal mean) had low CBF-AI<sub>s</sub> values (ranging from  $-0.82$  to  $-0.28$ ).

#### **Relation between Perfusion Status and Seizure Variables**

Low CBF-AI values ( $r = -0.58$ ,  $P = .03$ ) and decreased ipsilateral CBV ( $r = -0.55$ ,  $P = .04$ ) were found to correlate with a longer duration of epilepsy. No significant correlation was found between MTTs, MTT-AIs, and duration of epilepsy. Both rCBF and rCBV asymmetries (but not MTT parameters) also showed an inverse correlation with seizure frequency scores ( $r = -0.56$ ,  $P = .04$  and  $r = -0.63$ ,  $P = .02$ , respec-

tively). Duration of epilepsy and seizure frequency did not correlate with each other ( $P = .60$ ).  $A_{sz}$  did not correlate with any perfusion parameter ( $P > .2$  in all correlations).

#### **Discussion**

Our study provides a new perspective on quantitative relationships among brain WM perfusion, brain atrophy, and seizure severity in patients with SWS. Specifically, we demonstrated that 1) increased blood flow in the affected hemisphere seems to be a relatively common phenomenon in children with SWS, found in more than one-third of the present patient sample, especially in younger children; 2) WM hypoperfusion in the affected hemisphere is associated with a long history of epilepsy and more severe brain atrophy, suggesting a progressive deterioration of perfusion status over time, leading to brain tissue loss; and 3) a significant relationship exists between seizure frequency and severity of WM hypoperfusion, suggesting a link between low brain perfusion and chronic seizures in SWS. This is in contrast with the conventional notion that SWS pathology is mostly confined to gray matter or regions of anomalous venous drainage. Despite the relatively normal appearance on conventional MR imaging, our data show the importance of WM perfusion in structural changes and seizure severity. Meanwhile, we could not demonstrate that WM perfusion status was a robust predictor of cognitive functions or motor impairment. It should be noted, however, that most children in this study had relatively good cognitive functions, which made this statistical comparison less useful. Motor dysfunction is more likely related to localized abnormalities in WM regions encompassing motor pathways, as suggested by diffusion tensor imaging studies.<sup>6</sup>

The characteristic vascular malformation of SWS and its associated abnormalities have been well described in the literature and include a leptomeningeal angioma displacing normal superficial cortical veins, compensatory dilation of the deep venous system, ipsilateral choroid plexus hypertrophy, and subsequent development of atrophic and calcified cerebral cortex due to neuronal loss and astrogliosis.<sup>1,2,20-22</sup> Al-

though MR imaging signs of “accelerated myelination” have been described in infants with SWS,<sup>23</sup> only a few recent MR imaging studies focused on the significance of WM pathology by using quantitative volumetry<sup>3</sup> or water diffusion measurements.<sup>4–6</sup> MR imaging studies of cerebral perfusion performed in small groups of SWS patients demonstrated mostly decreased perfusion in regions with meningeal enhancement<sup>11,12</sup>; additional perfusion defects were seen in areas of deep venous abnormalities. Based on histologic studies, the cortical blood flow reduction was speculated to be secondary to the venous stasis and hypertension due to malformed cortical vessels as well as venous thrombosis.<sup>1,2,24,25</sup> Nevertheless, a SPECT study found hyperperfused cortex in some infants with SWS even before their first seizures.<sup>7</sup> A more recent MR imaging study also reported increased rCBF and rCBV of the affected cerebral tissue in 2 children with SWS and recent onset seizures.<sup>13</sup> Possible causes of increased perfusion in their studies included altered hemodynamics due to recent seizures; however, the exact mechanism leading to blood flow increases remained unclear. In our study, children with relative hyperperfusion in the affected WM had no recent seizures but were slightly younger and had milder brain atrophy, whereas those with decreased perfusion had more advanced disease with long duration of epilepsy and atrophy. This suggests that hyperperfusion is an interictal phenomenon and may represent a relatively early stage of pathology, possibly indicating ongoing hypoxic injury. Increased CBF on PWI has been indeed reported in neonates with hypoxic-ischemic encephalopathy<sup>26</sup>; changes involved the WM in some cases and were hypothesized to represent ongoing injury in reperfusion areas with abnormal cerebral autoregulation. Transient increase of glucose metabolism, also described in young children with hypoxic damage (due to both SWS and perinatal hypoxia), may be a metabolic aspect of the same phenomenon, possibly indicating hypoxia-induced, glutamatergic excitotoxic injury leading to subsequent tissue loss and hypometabolism.<sup>27–31</sup>

Our previous study showed a significant negative correlation between hemispheric WM volume and age in children with SWS.<sup>3</sup> Hypoxic injury due to impaired venous drainage of the affected hemisphere was considered as the putative mechanism causing early WM abnormalities.<sup>32</sup> The present PWI study provides further evidence for WM injury at the perfusion level with relation to age as well as brain atrophy. Decreased blood flow in brain tissue corresponding to the vascular abnormalities over time may aggravate the extent of hypoxic injury leading to progressive neuronal death, astrogliosis, and atrophy. Because blood flow changes can occur before structural abnormalities in SWS,<sup>10,11</sup> early perfusion abnormality may be a useful imaging marker to indicate imminent WM damage.

The results also have implications regarding the pathomechanism of seizures in SWS. The association of long duration of epilepsy and high seizure frequency with severe hypoperfusion suggests that chronic hypoperfusion and tissue hypoxia may play a role in seizure generation in SWS. In contrast, frequent seizures may contribute to brain ischemia and disease progression. The findings suggest that improved tissue perfusion may lead to better seizure control, whereas lower seizure frequency also may prevent progressive ischemic damage. Longitudinal studies could further elucidate the exact

causative relationship between brain perfusion status and seizure severity in SWS.

Several methodologic issues should be considered when interpreting our data. First, perfusion measurements may be affected to some extent by brain atrophy and cortical calcification in the affected hemisphere. This effect was largely diminished by carefully placing multiple ROIs in WM regions, avoiding cortex (where calcification is most likely and artifacts from blood flow changes from overlying angioma may confound accurate perfusion measurements from brain tissue) and also large vessels, so that the measured data reflect tissue perfusion. Moreover, calculation of brain atrophy asymmetry (BA-AI) included both gray matter and WM volume. It remains to be determined whether perfusion abnormalities affect gray and WM volumes differentially. Also, our control group included adults, and we relied on asymmetry measurements to define abnormal decreases and increases in the affected hemisphere. This approach seems to be valid, because it does not rely on measurement of absolute perfusion values, which undergo nonlinear changes during childhood (an early increase during the first 2–3 years of life and a gradual decrease during adolescence<sup>33,34</sup>).

## Conclusions

MR PWI of the affected cerebral WM indicates dynamic perfusion abnormalities in children with SWS: increased perfusion in mostly younger patients may represent a transient phenomenon, before severe brain atrophy occurs in the affected brain regions. Decreased perfusion is associated with high seizure frequency, long epilepsy duration, and brain atrophy, suggesting a detrimental effect of chronic seizures on brain structure and function. MR PWI is a helpful technique to quantitatively evaluate blood flow abnormalities at different stages of evolution of SWS.

## Acknowledgments

We are grateful to Yang Xuan, BS, for technical support in the MR imaging acquisition. We also thank Majid Khalaf, MD, Anne Deboard, RN, and Jane Cornett, RN, for assistance in sedation. We thank the Sturge-Weber Foundation for referring patients to us. We are also grateful to the families and children who participated in the study.

Disclosures: Yongquan Ye: *Research Support (including provision of equipment and materials)*; Wayne State University; Harry T. Chugani: *Consultant*; Novartis, Lundbeck.

## References

1. Comi AM. **Advances in Sturge-Weber syndrome.** *Curr Opin Neurol* 2006;19:124–28
2. Comi AM. **Pathophysiology of Sturge-Weber syndrome.** *J Child Neurol* 2003;18:509–16
3. Juhasz C, Lai Ch, Behen ME, et al. **White matter volume as a major predictor of cognitive function in Sturge-Weber syndrome.** *Arch Neurol* 2007;64:1169–74
4. Deary IJ, Bastin ME, Pattie A, et al. **White matter integrity and cognition in childhood and old age.** *Neurology* 2006;66:505–12
5. Juhasz C, Haacke EM, Hu J, et al. **Multimodality imaging of cortical and white matter abnormalities in Sturge-Weber syndrome.** *AJNR Am J Neuroradiol* 2007;28:900–06
6. Alkonyi B, Govindan RM, Chugani HT, et al. **Focal white matter abnormalities related to neurocognitive dysfunction: an objective diffusion tensor imaging study of children with Sturge-Weber syndrome.** *Pediatr Res Epub* 2010 Sep 17
7. Pinton F, Chiron C, Enjolras O, et al. **Early single photon emission computed tomography in Sturge-Weber syndrome.** *J Neurol Neurosurg Psychiatry* 1997;63:616–21

8. Duncan DB, Herholz K, Pietrzyk U, et al. **Regional cerebral blood flow and metabolism in Sturge-Weber disease.** *Clin Nucl Med* 1995;20:522–23
9. Maria BL, Neufeld JA, Rosainz LC, et al. **High prevalence of bihemispheric structural and functional defects in Sturge-Weber syndrome.** *J Child Neurol* 1998;13:595–605
10. Lin DD, Barker PB, Kraut MA, et al. **Early characteristics of Sturge-Weber syndrome shown by perfusion MR imaging and proton MR spectroscopic imaging.** *AJNR Am J Neuroradiol* 2003;24:1912–15
11. Evans AL, Widjaja E, Connolly DJ, et al. **Cerebral perfusion abnormalities in children with Sturge-Weber syndrome shown by dynamic contrast bolus magnetic resonance perfusion imaging.** *Pediatrics* 2006;117:2119–25
12. Lin DD, Barker PB, Hatfield LA, et al. **Dynamic MR perfusion and proton MR spectroscopic imaging in Sturge-Weber syndrome: correlation with neurological symptoms.** *J Magn Reson Imag* 2006;24:274–81
13. Oguz KK, Senturk S, Ozturk A, et al. **Impact of recent seizures on cerebral blood flow in patients with Sturge-Weber syndrome: study of 2 cases.** *J Child Neurol* 2007;22:617–20
14. Haacke EM, Ayaz M, Khan A, et al. **Establishing a baseline phase behavior in magnetic resonance imaging to determine normal vs. abnormal iron content in the brain.** *J Magn Reson Imag* 2007;26:256–264
15. Haacke EM, Mittal S, Wu Z, et al. **Susceptibility-weighted imaging: technical aspects and clinical applications, part I.** *AJNR Am J Neuroradiol* 2009;30:19–30
16. Kelley TM, Hatfield LA, Lin DD, et al. **Quantitative analysis of cerebral cortical atrophy and correlation with clinical severity in unilateral Sturge-Weber syndrome.** *J Child Neurol* 2005;20:867–70
17. Ostergaard L, Weisskoff RM, Chesler DA, et al. **High resolution measurement of cerebral blood flow using intravascular tracer bolus passages. Part I: Mathematical approach and statistical analysis.** *Magn Reson Med* 1996;36:715–25
18. Engel J Jr., Van Ness PC, Rasmussen TB, et al. **Outcome with respect to epileptic seizures.** In: Engel J Jr, ed. *Surgical Treatment of the Epilepsies*. 2nd ed. New York: Raven Press; 1993, 609–621
19. Shrout PE, Fleiss JL. **Intraclass correlations: uses in assessing raters reliability.** *Psychol Bull* 1979;86:420–28
20. Norman MG, Schoene WC. **The ultrastructure of Sturge-Weber disease.** *Acta Neuropathol (Berl)* 1977;37:199–205
21. Di Trapani G, Di Rocco C, Abbamondi AL, et al. **Light microscopy and ultrastructural studies of Sturge-Weber disease.** *Childs Brain* 1982;9:23–36
22. Simonati A, Colamaria V, Bricolo A, et al. **Microgyria associated with Sturge-Weber angiomatosis.** *Childs Nerv Syst* 1994;10:392–95
23. Adamsbaum C, Pinton F, Rolland Y, et al. **Accelerated myelination in early Sturge-Weber syndrome: MRI-SPECT correlations.** *Pediatr Radiol* 1996;26:759–62
24. Prayson RA, Grewal ID, McMahon JT, et al. **Leukocyte adhesion molecules and x-ray energy dispersive spectroscopy in Sturge-Weber disease.** *Pediatr Neurol* 1996;15:332–36
25. Cunha e Sá M, Barroso CP, Caldas MC, et al. **Innervation pattern of malformative cortical vessels in Sturge-Weber disease: an histochemical, immunohistochemical, and ultrastructural study.** *Neurosurgery* 1997;41:872–76
26. Wintermark P, Moessinger AC, Gudinchet F, et al. **Perfusion-weighted magnetic resonance imaging patterns of hypoxic-ischemic encephalopathy in term neonates.** *J Magn Reson Imaging* 2008;28:1019–25
27. Chugani HT, Mazziotta JC, Phelps ME. **Sturge-Weber syndrome: a study of cerebral glucose utilization with positron emission tomography.** *J Pediatr* 1989;114:244–53
28. Pu Y, Li QF, Zeng CM, et al. **Increased detectability of alpha brain glutamate/glutamine in neonatal hypoxic-ischemic encephalopathy.** *AJNR Am J Neuroradiol* 2000;21:203–12
29. Hagberg H, Thornberg E, Blennow M, et al. **Excitatory amino acids in the cerebrospinal fluid of asphyxiated infants: relationship to hypoxic-ischemic encephalopathy.** *Acta Paediatr* 1993;82:925–29
30. Blennow M, Ingvar M, Lagercrantz H, et al. **Early [<sup>18</sup>F]FDG positron emission tomography in infants with hypoxic-ischaemic encephalopathy shows hypermetabolism during the postasphyctic period.** *Acta Paediatr* 1995; 84:1289–95
31. Batista CE, Chugani HT, Juhasz C, et al. **Transient hypermetabolism of the basal ganglia following perinatal hypoxia.** *Pediatr Neurol* 2007; 36:330–33
32. Pfund Z, Kagawa K, Juhasz C, et al. **Quantitative analysis of gray- and white matter volumes and glucose metabolism in Sturge-Weber syndrome.** *J Child Neurol* 2003;18:119–26
33. Biagi L, Abbruzzese A, Bianchi MC, et al. **Age dependence of cerebral perfusion assessed by magnetic resonance continuous arterial spin labeling.** *J Magn Reson Imaging* 2007;25:696–702
34. Bjørnerud A, Emblem KE. **A fully automated method for quantitative cerebral hemodynamic analysis using DSC-MRI.** *J Cereb Blood Flow Metab* 2010;30: 1066–78